Available online at www.sciencedirect.com
ScienceDirect
Journal of Power Sources 177 (2008) 262–272
JOURNAL OF POWER SOURCES
www.elsevier.com/locate/jpowsour

Fabrication of novel proton exchange membranes for DMFC via UV curing

Chi-An Dai [a,b,*], Chien-Pan Liu [a], Yi-Huan Lee [b], Chun-Jie Chang [b], Chi-Yang Chao [c], Yao-Yi Cheng [d]

[a] *Department of Chemical Engineering, National Taiwan University, Taipei 106, Taiwan*
[b] *Institute of Polymer Science and Engineering, National Taiwan University, Taipei 106, Taiwan*
[c] *Department of Materials Science and Engineering, National Taiwan University, National Taiwan University, Taipei 106, Taiwan*
[d] *Institute of Organic and Polymeric Materials, National Taipei University of Technology, Taipei 106 Taiwan*

Received 5 November 2007; received in revised form 23 November 2007; accepted 23 November 2007
Available online 5 December 2007

Abstract

The radiation hardening of various UV curable resins provides a simple but powerful method to fabricate thin films or membranes with desirable physical and chemical properties. In this study, we proposed to use this method to fabricate a novel proton exchange membrane (PEM) for direct methanol fuel cells (DMFC) with good mechanical, transport and stability properties. The PEM was prepared by crosslinking a mixture of a photoinitiator, a bifunctional aliphatic urethane acrylate resin (UAR), a trifunctional triallyl isocyanate (TAIC) crosslinker and tertrabutylammonium styrenesulfonate (SSTBA) to form a uniform network structure for proton transport. Key PEM parameters such as ion exchange capacity (IEC), water uptake, proton conductivity, and methanol permeability were controlled by adjusting the chemical composition of the membranes. The IEC value of the membrane was found to be an important parameter in affecting water uptake, conductivity as well as the permeability of the resulting membrane. Plots of the water uptake, conductivity, and methanol permeability vs. IEC of the membranes show a distinct change in the slope of their curves at roughly the same IEC value which suggests a transition of structural changes in the network. It is demonstrated that below the critical IEC value, the membrane exhibits a closed structure where hydrophilic segments form isolated domains while above the critical IEC value, it shows an open structure where hydrophilic segments are interconnected and form channels in the membrane. The transition from a closed to an open proton conduction network was verified by the measurement of the activation energy of membrane conductivity. The activation energy in the closed structure regime was found to be around 16.5 kJ mol^{-1} which is higher than that of the open structure region of 9.6 kJ mol^{-1}. The membranes also display an excellent oxidative stability, which suggests a good lifetime usage of the membranes. The proton conductivities and the methanol permeabilities of all membranes are in the range of 10^{-4} to 10^{-2} S cm^{-1} and 10^{-8} to 10^{-7} cm^2 s^{-1}, respectively, depending on their crosslinking density. The membranes show great selectivity compared with those of Nafion®. The possibility of using this PEM for DMFC devices is suggested.

Keywords: DMFC; Proton exchange membranes; Proton conductivity; Methanol permeability; UV-curing

1. Introduction

Fuel cells have been paid an intensive attention due to their great potential for the production of clean electrical power with higher efficiencies than current power sources at a lower environmental cost. Among the various types of fuel cells, the liquid feed direct methanol fuel cells (DMFC) have been the focal point of development due to these power sources presenting a high-energy efficiency and low emission of pollutants [1–4]. The design of a DMFC is almost the same as that of a hydrogen feed polymer electrolyte membrane fuel cell (PEMFC), except for using different feeding fuel and catalyst. The cell performance of a DMFC system is usually lower than that of a PEMFC due to poor efficiency of catalyst [5]. However, PEMFC uses hydrogen as fuel which may cause some problems, such as production,

* Corresponding author at: Department of Chemical Engineering, National Taiwan University, Taipei 106, Taiwan. Tel.: +886 2 3366 3051.
E-mail address: polymer@ntu.edu.tw (C.-A. Dai).

0378-7753/$ – see front matter © 2007 Elsevier B.V. All rights reserved.
doi:10.1016/j.jpowsour.2007.11.097

storage and transportation of hydrogen gas. As fuel in DMFC, methanol, a liquid at room temperature, has limited toxicity, is cheap and has a high energy density (3800 kcal l^{-1}) compared to hydrogen at 360 atm (658 kcal l^{-1}) [6,7]. Consequently, DMFC are promising candidates for portable power applications (cell phones, laptops) or applications in automobiles (cars, trucks, buses) because of its lower weight, simple fueling (easy storage of methanol, no reformer required), low emissions and low temperatures [8,9].

Currently, perfluorosulfonic acid (PFSA) polymer membranes, such as Nafion® membranes (DuPont), are the major membranes used in the polymer electrolyte membrane fuel cells (PEMFCs) as well as in the DMFCs. PFSA membranes are composed of a hydrophobic carbon–fluorine backbone chains with perfluoroether side chains containing a strong hydrophilic sulfonic acid groups. For example, Nafion®-117, in particular, are the most commonly used membrane as they are readily available, have good mechanical strength and stability. However, some of the drawbacks, such as high cost ($500 USD m^{-2}), stability problem at high temperature, poor barrier to methanol crossover [10] and difficulty in the synthesis and processing [11–14]. In addition, when the methanol crossover occurs, unreacted methanol passes through the PEM and reacts directly at the cathode catalyst. This causes a serious reduction of DMFC voltage and results in catalyst poisoning and mixed potential loss at the cathode [15]. In brief, the methanol crossover causes tremendous reduction of the overall efficiency. Therefore, it is necessary to develop an alternative membrane with less expensive and low methanol permeability and high performance. Currently, a number of sulfonic acid containing random copolymers have been synthesized for the DMFC in recent years. Sulfonated poly(styrene) (SPS), a random copolymer of poly(styrene) and poly(styrene sulfonic acid) (PSSA) has been investigated for its use in the DMFC [16–19]. Membranes made from the copolymers were one of the first PEMs deployed for the space program in the early 1960s [20,21].

The technology of UV curing is based on formulations which usually consist of oligomer resins, monomers and photoinitiators. In order to develop a UV formulation that can be used in DMFC as PEM, sulfonate functional groups, the best proton transporting chemical moiety, need to be incorporated in the formulation [22,23]. The simplest vinylic monomer with sulfonate functional group which is also commercially available is sodium styrene sulfonate (SSNa). In principle, to develop a UV cured formulation for PEM can be made by simply mixing a UV curable resin with sodium styrene sulfonate monomer to offer the proton transporting property to the resulting resin. However, sodium styrene sulfonate is a solid at the room temperature and is not soluble in most UV curable resins. Mechanical mixing of the solid material with UV curable resin results in an inhomogeneous macroscopically phase separated proton exchange membrane.

In this study, we prepare UV-curable interpenetrating polymer networks based on crosslinking a mixture of bifunctional urethane acrylate resin (UAR) and trifunctional triallyl isocyanate (TAIC) as a matrix membrane grafted with monomeric styrene sulfonate as proton conduction moiety. In order to solve the above mentioned problem in the previous paragraph, solid sodium styrene sulfonate is modified with a quaternary ammonium salt, tetrabutylammonium hydroxide. By replacing sodium with tetrabutylammonium, tetrabutylammonium styrene sulfonate is a liquid at the room temperature which can be easily mixed with UV curable resin at the molecular level which facilitates the completion of UV curable formulation for PEM. The quaternary ammonium can be removed with successive washing with sodium hydroxide. In this study, we have used a aliphatic urethane acrylate as the resin matrix which is known to offer a wide range of excellent application properties, such as high impact and tensile strength, abrasion resistance and toughness combined with excellent chemical, photochemical and solvent resistances [24–26]. The structure of the resulting membrane is therefore a interpenetrating polymer networks (IPN) with good proton transport and stable dimensional stability. In addition, the crosslinking degree and the amount of sulfonate functional group were controlled to seek the best performance in terms of methanol permeability and proton conductivity measurements.

2. Experimental

2.1. Materials

Sodium styrene sulfonate (SSNa) was purchased from Aldrich. Phenolphthalein (indicator grade, pure), tertrabutylammonium hydroxide (40%), acetone (99%), triallyisocyanurate (TAIC) and sulfuric acid (98%) were all obtained from Acros. Aliphatic urethane diacrylate resin was supplied by the Double-Bond Chemical Co. of Taiwan. The precursor polyol of the resin is poly(propylene oxide) and the resulting chemical structure of the resin is shown in Fig. 1(a). The characteristics of the resin is shown in Table 1. The photoinitiator, 1-hydroxycyclohexyl phenyl ketone (Irgacure® 184) was supplied by Ciba Specialty Chemicals.

2.2. Synthesis of tertrabutylammonium styrene sulfonate (SSTBA) from SSNa

Tertrabutylammonium styrenesulfonate (SSTBA) was prepared from SSNa using a reaction scheme shown in Fig. 1b. Seven grams of SSNa was solubilized in water. One molar equivalent of tetrabutylammonium hydroxide was added dropwise in water at the ambient temperature. Extraction with 80 ml of CH_2Cl_2 (several times) then drying the organic layer on $MgSO_4$ and evaporating under vacuum lead to a yellow viscous liquid in 98% yield. Proton NMR was used to verify to stochiometric amount of the SSTBA as shown in Fig. 1c.

2.3. Membrane preparation

The UV-curable membrane system for DMFC consisted of four components: a photopolymerizable oligomer, a crosslinker, a functional monomer, and a photoinitiator [24]. The oligomer we used was a bifunctional aliphatic urethane diacrylate oligomer and the functional photopolymerizable monomer was SSTBA. Irgacure® 184 was used as a photoinitiator and the

Table 1
The transport properties of the UV cured membranes compared with those of IEC, water uptake (WU), the state of water, and number of water molecules per ionic site (—SO_3H) in different polymer membranes compared with those of Nafion®-117

Membrane code	IEC (meq g^{-1})	WU[a] (%)	FW[b] (%)	BW[c] (%)	BW/FW	λ_w[d]
SSNa/UAR/TAIC(2/2/0.5)[e]	1.05	36.0	12.0	24.0	2.0	19.2
SSNa/UAR/TAIC(2/2/1)	1.12	31.3	10.3	21.0	2.1	15.5
SSNa/UAR/TAIC(2/2/2)	1.17	28.6	9.3	19.3	2.1	13.6
SSNa/UAR/TAIC(2/2/3)	1.23	25.3	8.2	17.1	2.1	11.4
SSNa/UAR/TAIC(2/2/4)	1.17	21.4	6.9	14.5	2.1	10.2
SSNa/UAR/TAIC(2/2/5)	1.08	17.1	5.5	11.6	2.1	8.8
SSNa/UAR/TAIC(2/2/6)	0.84	14.7	4.7	10.0	2.2	9.7
Nafion®-117	0.9	33.4	7.8	25.7	3.31	20.6

[a] Water uptake or total water content.
[b] Free water, which is calculated from the DSC analysis.
[c] Bound water = total water content-free water.
[d] λ_w: number of water molecules per ionic site.
[e] The numbers in parenthesis stands for the weight fraction for the corresponding constituents in the UV curable formation.

weight added in the formulation was adjusted to 10% of the total weight. In addition, a trifunctional crosslinker, triallyl isocyanate (TAIC) was added in the formulation in order to form a network structure in the membrane. All of these chemicals were mixed together by varying each component composition and stirred continuously until the solution to form a homogeneous mixture at room temperature. Membranes were prepared by casting the mixed solution onto a glass plate using a Gardner coating knife with predetermined drawdown thickness then irradiated with 2106 mJ cm^{-2} UV light. The thickness of all membranes was kept to be around 140 μm. Before tests, all samples were soaked in a large volume of 1 M HCl solution, heated to 70 °C for 2 h and subsequently placed in a 1 M NaCl solution, heated to 40 °C in order to replace tertrabutylammonium with sodium ion. The resulting membranes were soaked in distilled water to obtain free standing membranes.

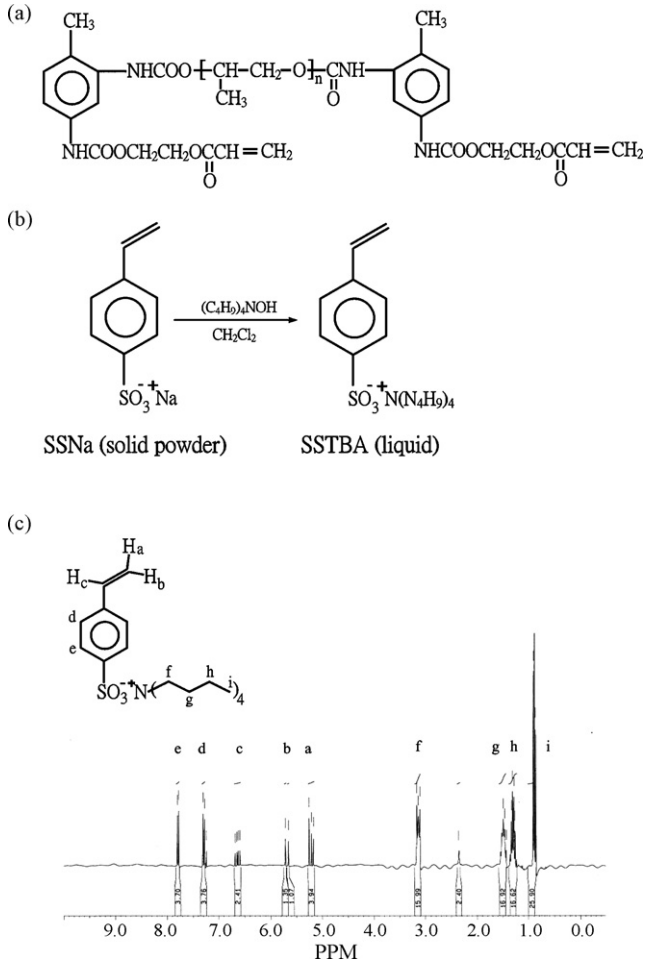

Fig. 1. (a) The chemical structure of the aliphatic urethane acrylate resin used in the study. (b) The synthesis scheme of the sulfonic acid graftable monomer, tertrabutylammonium styrenesulfonate (SSTBA). (c) The NMR spectrum of SSTBA shows the stoichiometric amount of the respective protons.

2.4. The swelling properties of the membranes

The membrane swelling towards pure water and methanol was determined in terms of conventional water uptake and the number of liquid molecular per sulfonate groups. The water uptake was determined in the following way: at first the membrane samples were dried under vacuum for 1 h at 80 °C and then weighed. They were then soaked in deionized water for 2 days until swelling equilibrium was achieved. The soaked membrane was carefully blotted with a filter paper to remove water on the surface followed by weight measurement. The water uptake was conducted measuring the weight differences between the fully hydrated membranes and the dried membranes. The water uptake was calculated by the following expression:

$$\mathrm{WU}\,(\%) = \frac{W_{\mathrm{swollen}} - W_{\mathrm{dry}}}{W_{\mathrm{dry}}} \times 100 \quad (1)$$

where W_{swollen} is the weight of water-swollen membranes and W_{dry} the weight of the dry membranes. The number of the absorbed water molecules per ionic site (λ_m or λ_w) was calculated using the following equations [27]:

$$\lambda_w = \frac{\mathrm{WU}}{M(18) \times \mathrm{IEC}} \times 1000 \quad (2)$$

where WU is the weight of the water uptake of the membrane samples, which is obtained from Eq. (1) and M the molecular weight, 18 g mol^{-1} of the considered liquid.

2.5. Ion exchange capacity

The ion exchange capacity (IEC) of the membranes was determined the conventional titration technique. First, a square piece of each membrane were soaked in a large volume of 1 M HCl solution and heated to 70 °C for 1 h. The samples were then washed with distilled water several times to remove excess HCl. In the next step, the samples were placed in a 50 ml of 1 M NaCl solution, heated to 40 °C and equilibrated for at least 24 h to replace the protons with sodium ions. The remaining solution was titrated with 0.01 N NaOH solution using phenolphthalein as an indicator. The IEC value (mmol g^{-1} or meq g^{-1}) was calculated using the following equation:

$$\mathrm{IEC} = \frac{0.01(V_O - V_E)}{W_{dry}} \tag{3}$$

where V_O is the volume of NaOH in the flask at the beginning of the titration, V_E is the volume of NaOH after equilibrium, and W_{dry} is the weight of the dry membrane (g).

2.6. Proton conductivity

Proton conductivity was determined by an electrochemical impedance spectroscopy (EIS) taken between 100 kHz and 0.1 MHz at a voltage amplitude of 10 mV using an impedance/gain-phase analyzer (Solartron 1260) in combination with an electrochemical interface (Solartron 1287). A homemade two-point probe electrode method was employed to measure the proton conductivity in the thickness direction of the membranes as shown in Fig. 2. The proton conductivity (σ) was obtained using the following equation:

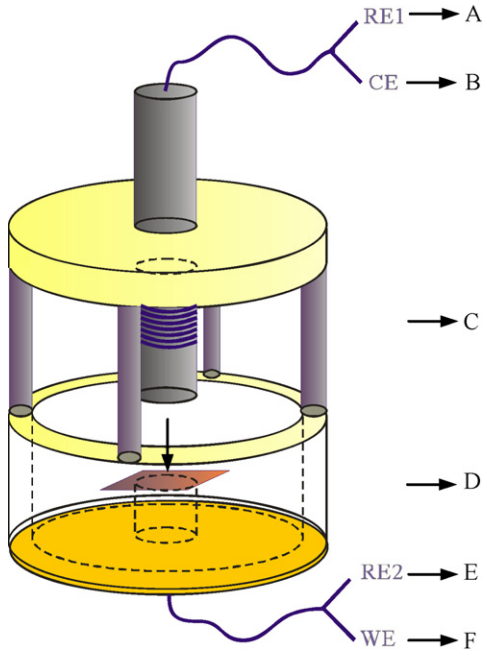

Fig. 2. Schematic diagram of the cell used for conductivity measurement in the thickness direction of the membrane sample: (A): reference electrode 1; (B): counter electrode; (C): spring; (D): membrane samples; (E): reference electrode 2; (F): working electrode.

$$\sigma = \frac{l}{RA} \tag{4}$$

where σ is the proton conductivity (S cm^{-1}) and l is the thickness of the membrane (cm). R is the bulk resistance or Ohmic resistance of the membrane sample (Ω). A is the contact area required for a proton to penetrate the membrane (cm^2). The impedance of each sample was measured at least five times to ensure data reproducibility.

2.7. Methanol permeability

The methanol permeability of the membranes was determined using a diaphragm diffusion cell method [28–30]. Basically, a glass cell consisted of two reservoirs each approximately 60 ml, separated by a vertical membrane. The membrane (effective area 3.14 cm^2) was fixed and clamped between both reservoirs. Initially, one reservoir (V_A) was filled with a 40 ml of 50 vol% methanol solution in distilled water, and the other reservoir (V_B) was filled with pure deionized water. Methanol permeates across the membrane by the concentration difference between the two reservoirs. We can measure the concentration of methanol by density/concentration meter (DMA4500, Anton Paar, Austria), then the methanol concentration in the receiving reservoir as a function of time is given by the following equation:

$$C_B = \frac{A}{V_B}\frac{DK}{l}[C_A(t_0)](t - t_0) \tag{5}$$

where C_B is the concentration of methanol in the water reservoir as time goes by, C_A the methanol concentration in the methanol reservoir, A (cm^2) the effective area of membrane, l (cm) the membrane thickness, V_B the volume of water in its reservoir, D the methanol diffusivity and K is the partition coefficient between the membrane and the adjacent solution. The product DK means the membrane permeability (P_M):

$$P_M = DK = \frac{1}{A}\frac{C_B(t)}{C_A(t_0)}\frac{V_B\, l}{t - t_0} \tag{6}$$

Parameter t_0 is the lag time corresponding to the time necessary for the methanol to pass through the membrane. C_B here is measured several times during the permeation experiment and the methanol permeability is obtained from the slope of equation (6).

2.8. Oxidative stability

Oxidative stabilities were determined using the Fenton's reagent (30 wt.% H_2O_2 solution containing 30 ppm $FeSO_4$) at 30 °C. The membranes were immersed in Erlenmeyer flask containing the Fenton's reagent which was pit in a water bath of 30 °C. The flask was shaken constantly until the membrane began to break. The times from commencement to break of samples were recorded.

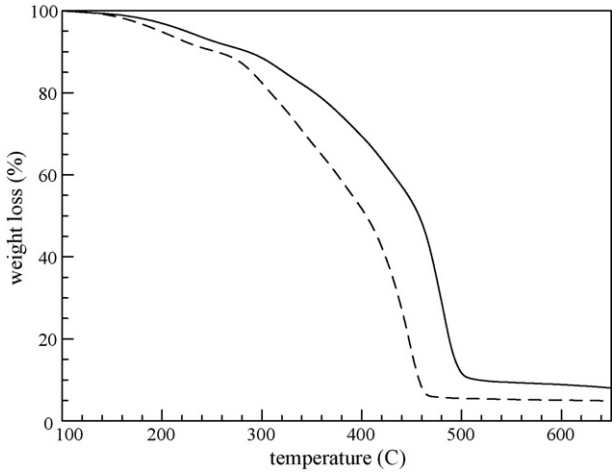

Fig. 3. TGA thermograph of the UV cured membranes (—) SSNa/UAR/TAIC (2/2/6) and (– – –) SSNa/UAR/TAIC (2/2/1).

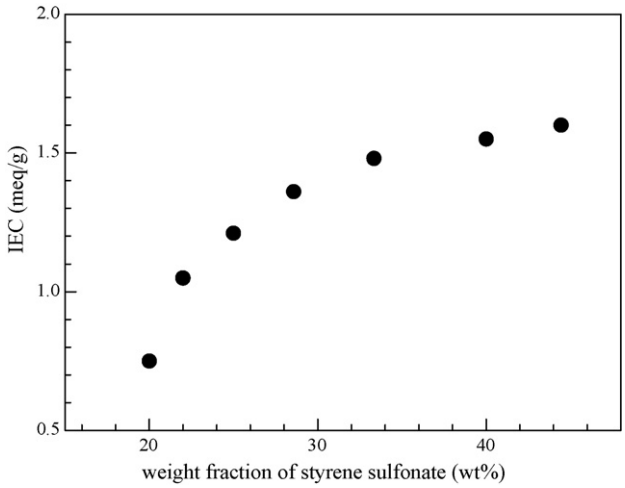

Fig. 4. IEC of SSNa/UAR/TAIC membranes plotted as a function of SSNa content in the membrane.

3. Results and discussion

3.1. Thermal and mechanical properties

Two types of the UV cured membranes with different crosslink density and amount of styrene sulfonate were examined by the thermogravimetric ananlysis (TGA). The TGA measurement was conducted in a nitrogen atmosphere from 50 to 700 °C at a heating rate of 10 °C min^{-1}. As shown in Fig. 3, the TGA thermograms of SSNa/UAR/TAIC(2/2/6) and SSNa/UAR/TAIC(2/2/1) membranes reveal three main weight loss regions. The weight loss arises from the process of thermal salvation, thermal desulfonation, and thermooxidation of the polymer matrix with increasing temperature. In the temperature range 50–100 °C, water desorption occurred (3–5%). From 170 to ∼270 °C, the weight loss proceeds via desulfonation of $–SO_3$ groups (5–8 wt.%), follows by a major degradation of cross-linking bridge and polymer backbone through 400–500 °C. The SSNa/UAR/TAIC(2/2/1) membrane shows larger weight loss resulted from desulfonation and a lower onset of thermal oxidation of the polymer matrix than that the SSNa/UAR/TAIC(2/2/6) membrane. The char yield (residual ash at 600 °C) after matrix decomposition shows that the highly crosslinked SSNa/UAR/TAIC(2/2/6) membrane is larger than that of SSNa/UAR/TAIC(2/2/1) membrane. These results show a general trend that higher crosslinked polymer matrix exhibit better thermal stability.

3.2. Transport properties

Since the ion exchange capacity (IEC) values are known to have a profound effect on the transport properties of proton exchange membranes. We first examine their IEC values of the membranes used in this study. The IEC values of the UV cured membranes were measured by the neutralization titration method described in Section 2 and listed in Table 1. Fig. 4 shows the variation of the IEC value as a function of SSNa weight fraction of the membrane. The IEC value increases with increasing weight fraction of SSNa added in the membrane. However, the increase in IEC decreases slightly with increasing SSNa amount. This decrease may be attributed to the increase amount of UAR resin as well as the decrease in the amount of TAIC added in the membrane, resulting in the changes of membrane morphology and internal structure. Such effect will be examined later in the section.

It is found in the literature that a threshold amount of matrix water was found to be required to maintain proper IEC and proton conductivity. On the other hand, excessive water uptake will induce undesired side effects and result in membrane swelling, mechanical frailty, low dimensional stability and high methanol permeability, all of which will lead to poor performance, especially in DMFC applications [31]. Maintaining an appropriate water uptake level is indispensable to ensure superior proton conductivity and to simultaneously reduce undesirable side effects. We compared the area-change ratio of the two membranes: SSNa/UAR/TAIC(2/2/1) and SSNa/UAR/TAIC(2/2/6). For membrane SSNa/UAR/TAIC(2/2/6), its area-change ratio (15%) is smaller than that (24%) of SSNa/UAR/TAIC(2/2/1). It is not surprising that with increasing crosslink density, SSNa/UAR/TAIC(2/2/6) shows less swelling in terms of change in the surface area compared with SSNa/UAR/TAIC(2/2/1). For Nafion-117, the area-change ratio was also measured to be around 24%. SSNa/UAR/TAIC(2/2/6) show less area-change ratio than that of Nafion. This is mainly due to its stable crosslinking structure.

Fig. 5 shows the variation in the water uptake of the membrane as a function of IEC value of the UV cured membranes. The membranes show a general trend that the water uptake increases with increasing IEC. The water uptake of the membranes increases roughly linearly with increasing IEC for IEC < 1.3 mmol g^{-1}. Notably, there is a change in the slope of the increase in the water uptake of the membrane for IEC > 1.3 mmol g^{-1}. Above 1.3 mmol g^{-1}, the water uptake value increases linearly with increasing IEC. The physical reason that an increase in the WU of the membrane with increasing

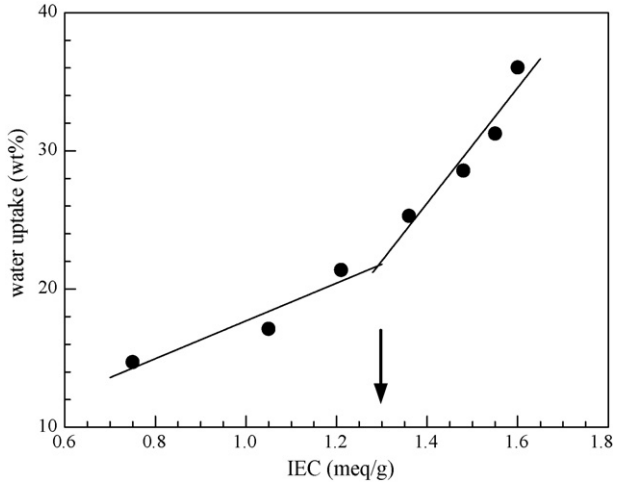

Fig. 5. Water uptake of SSNa/UAR/TAIC membranes as a function of SSNa content in the membrane. (●) Measurements from the water uptake experiment and (—) the line is to guide the eyes. The arrow indicates that a transition of water uptake vs. IEC occurs.

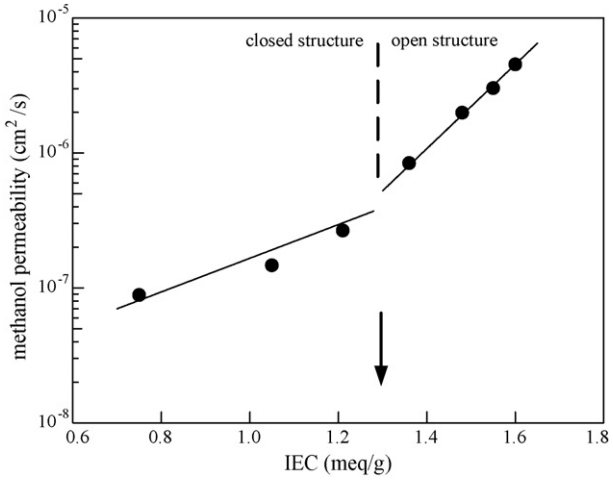

Fig. 6. Methanol permeability of SSNa/UAR/TAIC membranes as a function of SSNa content in the membrane. (●) Measurements from the methanol permeability experiment and (—) the line is to guide the eyes. The arrow indicates that a transition from a closed structure to an open one for methanol permeability occurs at IEC = 1.3 meq g^{-1}.

IEC is two-folds. With increasing IEC, the amount of TAIC crosslinker added in the membrane is decreased which substantially decreases the crosslink density. In addition, the amount of styrene sulfonate functional group which is highly hydrophilic increases, leading to a dramatic increase in the water uptake. The existence of a transition at which the way the membrane absorb water indicate that a structure change upon changing the relative amount of SSNa, UAR and TAIC in the UV cured membrane. McGrath and coworkers [20] had showed experimentally that a similar transition of water uptake vs. degree of sulfonation of their ion-conductive polymer occurred. They demonstrated that the correct way to link all major PEM transport properties together is to relate them to the IEC value of their membrane. By plotting the water uptake, methanol permeability, and proton conductivity vs. their IEC value, they further showed this slope-changing transition was associated with a change in their network structure from closed to open [32]. The observed transition in our system appears to be similar to the one observed in their system.

To further verify such a transition, we examine the dependence of the methanol permeability vs. IEC in our UV cured membranes. The steady-state fluxes through the UV cured membranes were verified using a diffusion-cell method. Fig. 6 shows the methanol permeability in unit of $cm^2\,s^{-1}$ as a function of membrane's IEC. The methanol permeability of the membranes was found to increase with increasing IEC. Similar to the water uptake property, the methanol transport property of the membranes shows a change in the slope of permeability vs. IEC. The transition was found to be at the same IEC (=1.3 meq g^{-1}) as the one in water uptake experiment, which indicates similar physics governing the transport property of the membrane. Beside the discovery of a transition, the methanol permeability values of all SSNa/UAR/TAIC membranes are lower than that of a commercially available Nafion®-117 membranes ($3.68 \times 10^{-6}\,cm^2\,s^{-1}$), except for the lowest crosslinked membrane of SSNa/UAR/TAIC(2/2/0.5).

The proton conductivity of the UV cured membrane is plotted as a function of IEC of the membrane as shown in Fig. 7. We found a slightly different trend of proton conductivity with respect to IEC. The proton conductivity increases with increasing IEC, reaches a maximum at the same transitional IEC (=1.3 meq g^{-1}) and finally reduces to a lower value. The proton conductivity was found to be a complex function of both IEC, water uptake, and as well as the state of water for ion conduction. Okada and coworkers have observed a similar behavior when they plot the conductivity as a function of the amount of sulfonate group [33]. The conductivity increases, reach a maximum, and drop to a lower value with increasing sulfonate group. Both in their case and in ours, the decreases in the proton conductivity were due to the dilution effect of charge carriers, resulted

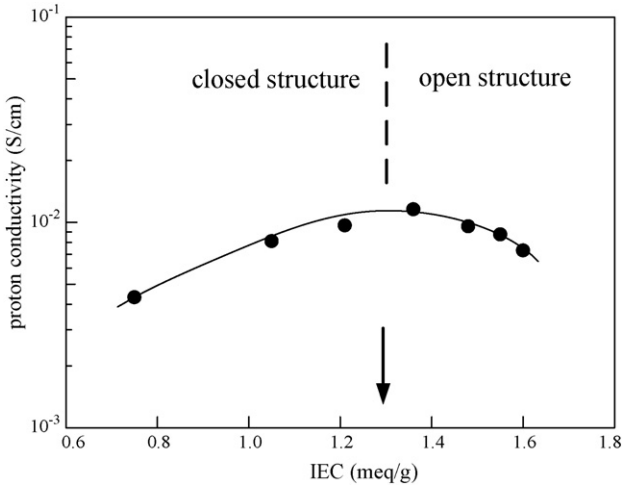

Fig. 7. Conductivity of SSNa/UAR/TAIC membranes as a function of SSNa content in the membrane. (●) Measurements from the conductivity experiment and (—) the line is to guide the eyes. The arrow indicates that a transition occurs at IEC = 1.3 meq g^{-1}.

from a substantial increase in the water uptake at high IEC value (>1.3 meq/g).

Generally, proton conductivity increases with increasing water uptake because a large free volume contributes to the high mobility of free ions. Also, proton conductivity increases with an increase in IEC because of the high charge density of the membranes. Therefore, proton conductivity is a function of both IEC and water uptake. In addition, it is also affected by the density of hydrophobic groups and the cluster of hydrophilic groups. Usually these membranes contain interpenetrating domains of both hydrophilic regions and hydrophobic ones. The hydrophobic domains formed with high crosslink density provide the hydrated PEMs with good mechanical strength, whereas the hydrophilic domains contain the hydrophilic ionic clusters such as sulfonate groups ensuring proton conduction. The existence of the two regions may lead to a microphase-separated structure, which will determine the proton conductivity of the membranes. When the sulfonation degree increases, these sulfonic groups ionic clusters aggregate more, the relative hydrophilic domains may expand and lead to a proper distribution of ion channels with good connectivity and protons can be fast transported in these channels (i.e., SSNa/UAR/TAIC(2/2/1) membranes). For SSNa/UAR/TAIC(2/2/6) membranes showed a much more microphase-separated structure. The mobility of the ionic clusters in the membranes will be more restricted, which lead to a low proton conductivity ability. Consequently, the more hydrophobic groups may decrease the performance of proton conductivity with high water uptake, so the hydrophobic groups should be well designed.

Based on the above three different measurements (water uptake, methanol permeability and conductivity), the same transition IEC value was observed. This result demonstrated that a fundamental structural change occurred in the membrane. It is therefore confirmed that below IEC < 1.3 meq g^{-1}, the network exhibits mainly closed structure while above IEC > 1.3 meq g^{-1}, the network exhibits an open structure. Difference in the film morphology was observed using field-emission SEM. As shown in Fig. 8, SSNa/UAR/TAIC(2/2/6) exhibit a much different side view of the memabrane compared with that of SSNa/UAR/TAIC(2/2/1). The SSNa/UAR/TAIC(2/2/1) membrane show much uniform film side-view compared with that of a higher crosslinked SSNa/UVR/TACI(2/2/6) indicating a brittle fracture surface.

3.3. State of water in the membranes

The state of water in particular has a strong influence on proton transport properties. Usually water in the membrane exists in two types: freezing bound water or free water (FW) and non-freezing bound water, or bound water (BW). When a small volume of water is absorbed into a polymer, the water molecules primarily associate with the polar and ionic groups present in the polymer chain. At a certain volume of absorbed water, the polar and ionic groups become saturated. The maximum volume of bound water is typically dependent on the polarity and the content of ionic groups in the polymer [34]. Free water is not bound to the polymer and shows the same temperature

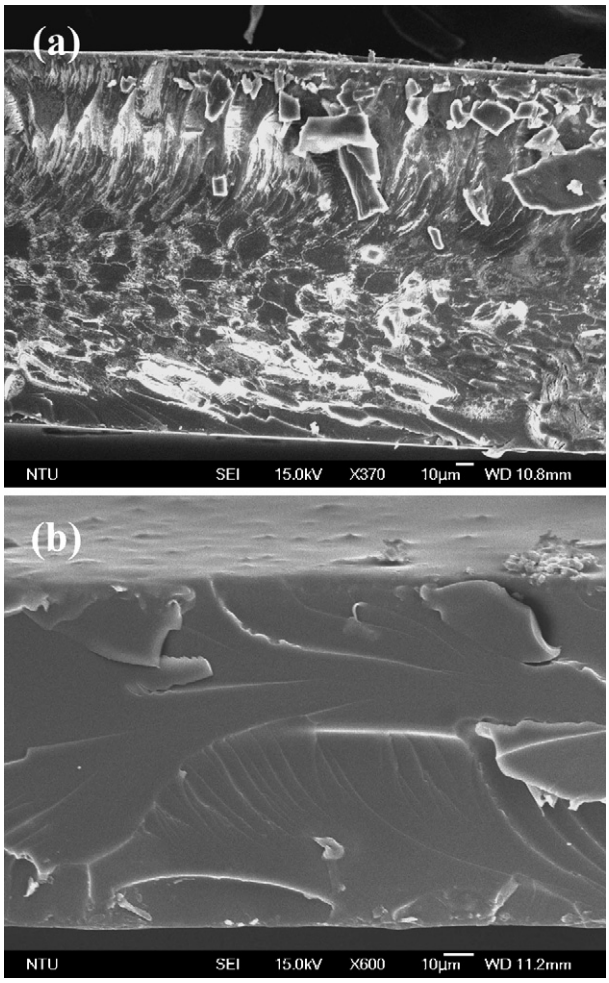

Fig. 8. FE-SEM cross-section image of prepared membranes (a) SSNa/UAR/TAIC(2/2/6) and (b) SSNa/UAR/TAIC(2/2/1).

and enthalpy of melting/crystallization as bulk water (i.e., 0 °C) [35,36]. Freezing bound water is defined as water that has a phase transition temperature less than 0 °C due to weak interaction such as hydrogen bonding with the hydrophilic groups in the polymer. Non-freezing bound water is defined as water that has no detectable phase transition from −73 to 0 °C because of strong interaction with the associate groups (i.e., sulfonic acid groups in the current case) of the polymer [37,38]. A series of water-swollen polymer membranes prepared in the present study containing a large amount of water in their networks. It demonstrated the water sorption characteristics and physicochemical properties depending not only on the water content but also on the state of water.

In this study, the DSC measurement was carried out to determine the amount of free water that is not bounded by the hydrogen bonding. The free water fraction of total water content is evaluated as the ratio of the endothermic peak area at around 0 °C for the water-swollen membranes to the melting endothermic heat of fusion for pure water, using the following equations:

$$m_{\text{free}} = \frac{\Delta H_{\text{free}}}{Q_{\text{melting}}} m_{\text{total}} \tag{7}$$

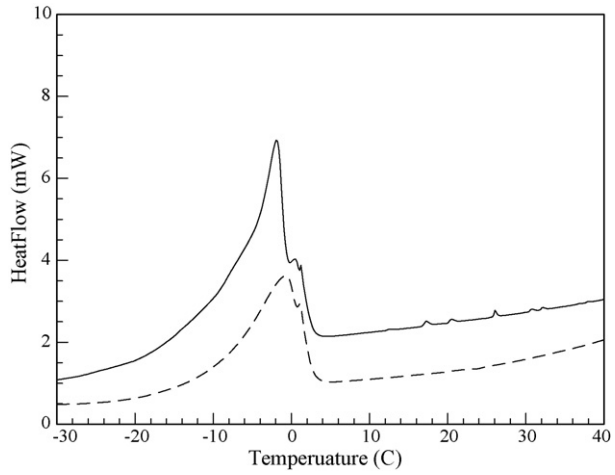

Fig. 9. DSC thermogram of (—) SSNa/UAR/TAIC(2/2/1) and (– – –) SSNa/UAR/TAIC(2/2/6).

The heat of melting, ΔH_{free}, of free water was determined from the area below the corresponding DSC peak and $Q_{melting}$ was known to be equal to 334 J g^{-1}. Bound water arising from the sulfonic acid groups (–SO_3H) is expressed as the difference between the total water and the free water content. Table 1 lists the water content corresponding to free water and bound water in different polymer membranes. The DSC thermograms for SSNa/UAR/TAIC(2/2/1) and SSNa/UAR/TAIC(2/2/6) membranes were compared as shown in Fig. 9. Based on the area under the melt endotherm, we found that per weight basis SSNa/UAR/TAIC(2/2/6) sample has less free water than that of SSNa/UAR/TAIC(2/2/1). The result is again due to the increase in the crosslink density which results in the decrease in the amount of free water available in the network structure.

There are more bound water existed in the network than the free water as shown in Table 1 (BW/FW ratio). This result is similar to that of Nafion-117, however, the value is lower than that of Nafion. As shown in Table 1, the total water content decreases with increasing amount of TAIC crosslinker, due to the increased degree of cross-linking of the membranes. This makes the polymer structure more compact and rigid, and results in a decrease in the free volume capable of containing water molecules. In addition, SSNa serving as "bound-water reservoirs" owing to its sulfonate groups. We calculated the number of water molecules per ionic site (λ_w) and found that with decreasing crosslinking density, λ_w increases continuously and finally reach a value close to that of Nafion-117.

3.4. Temperature dependence of proton conductivity

It is demonstrated that the content of hydrophilic components and their distribution in the matrix of the membrane play a key role in proton conductivity. The high proton conductivity can be attributed to the hydroxyl and sulfonic acid groups present in the PEM, which give rise to hydrophilic regions in the polymer because of their strong affinity toward water. These hydrophilic areas formed around the cluster of side chains lead to absorption of water, enabling easy proton transfer [39]. Since the proton conductivity of a PEM is generally thermally stimulated, it is natural to expect a rise in proton conductivity with temperature. The AC impedance spectra (i.e., Nyquiest plot) for both SSNa/UAR/TAIC(2/2/1) and SSNa/UAR/TAIC (2/2/6) polymer membranes are shown in Fig. 10(a) and (b), respectively. Additionally, the bulk resistance R_b (Ω) for the polymer membranes can be analyzed from above AC impedance spectra.

The temperature dependence of proton conductivity for SSNa/UAR/TAIC(2/2/6), SSNa/UAR/TAIC (2/2/1) polymer membranes and Nafion®-117 membrane samples are compared in Fig. 11. The Arrhenius plot in Fig. 11 is an indication of the mechanism of proton transport, which follows the Arrhenius relationship $\sigma = \sigma_0 \exp(-E_a/kT)$ in the tested temperature range from 25 to 80 °C. From the plot, the activation energy can be calculated, which shows that the proton conductivity mechanism through the proton exchange membrane have occurred via two routes. One is a hopping or Grotthuss mechanism, in which a proton passes down the chain via highly ionic conductive functional groups such as sulfonate groups; and the other is a vehicle (segmental motion) mechanism, in which a proton combines with a vehicle, such as H_3O^+ or $CH_3OH_2^+$ and an unprotonated vehicle (such as H_2O), which allows the net transport of protons [40,41]. It is believed that the bound water participates by the Grotthuss mechanism, and

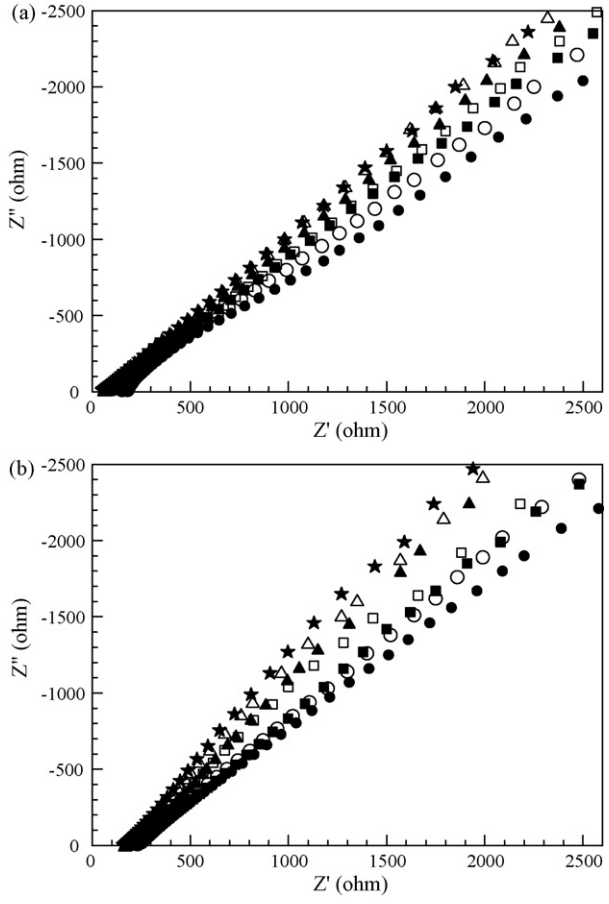

Fig. 10. Nyquiest plot of (a) SSNa/UAR/TAIC(2/2/1) polymer membrane and (b) SSNa/UAR/TAIC(2/2/6) polymer membrane. (●) 25 °C, (◯) 30 °C, (■)40 °C, (□)50 °C, (▲)60 °C, (△) 70 °C, and (⋆) 80 °C.

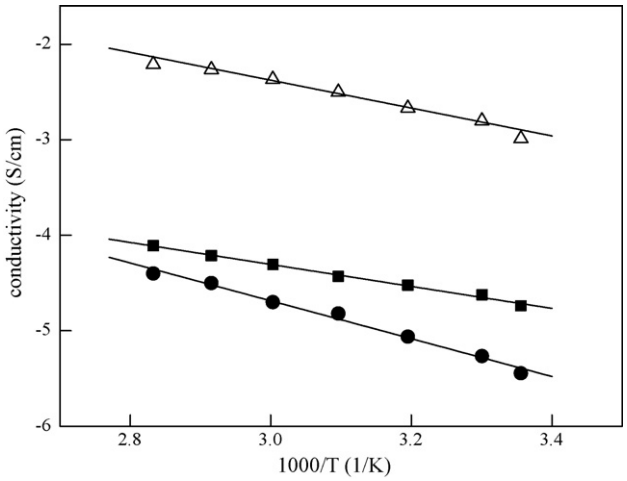

Fig. 11. The Arrhenius plot of conductivity as a function of temperature for (△) Nafion-117, (■) SSNa/UAR/TAIC(2/2/1), and (●) SSNa/UAR/TAIC(2/2/6).

the free water takes part mostly by vehicle mechanism [42]. The bound water facilitates the proton transport ability through the Grotthuss mechanism, originating by generation of a continuous proton conductive pathway. Therefore, the higher proton conductivity for the SSNa/UAR/TAIC(2/2/1) polymer membrane than SSNa/UAR/TAIC(2/2/6) polymer membrane can be due to the higher bound water contents in the membrane. The apparent activation energies (E_a) for proton conduction that were determined from the slops of the Arrhenius plots in the SSNa/UAR/TAIC(2/2/1) polymer membrane and SSNa/UAR/TAIC(2/2/6) polymer membrane found to be 9.6 and 16.5 kJ mol^{-1}, respectively. In the Nafion®-117, the activation energy, E_a we measured was about 10.79 kJ mol^{-1} which is between with above two kinds of membrane. It should be noted that E_a is a measure of how easily proton conduction occurs. Lower values of E_a indicate that proton conductivity occurs readily and the barriers to proton conduction are low, whereas a higher E_a indicates that protons do not move as easily through the polymer [43]. It is known that the Grotthuss mechanism requires low activation energy than the vehicle mechanism [38]. The activation energy values from the Nafion®-117 can be proved that the proton transport might have occurred by both the Grothuss mechanism and predominantly by the vehicular mechanism. Hence, it can be concluded from the Arrhenius plot that the SSNa/UAR/TAIC(2/2/6) polymer membrane has larger value of E_a and the great part of proton transport is by vehicle mechanism. This coincides with the fact that the SSNa/UAR/TAIC(2/2/6) polymer membrane has a closed structure with high crosslinked obstacle to hinder proton conduction. However, SSNa/UAR/TAIC(2/2/1) polymer membrane even has lower value of E_a to easily transfer proton through membranes, indicating the existence of its open ion conduction open structure. Based on the above data, a schematic representation of the membrane morphology is proposed and drawn in Fig. 12(a) and (b) to demonstrate the structural transition for proton conduction.

3.5. Selectivity of the membrane

High methanol crossover is a big problem for the commercialization of Nafion membrane in fuel cell applications. The ideal PEM performance in DMFC is expected to have high proton conductivity and low methanol permeability. Therefore, the ratio of proton conductivity to methanol permeability or selectivity (Φ) is also important parameter for PEM evaluation. It can be noticed

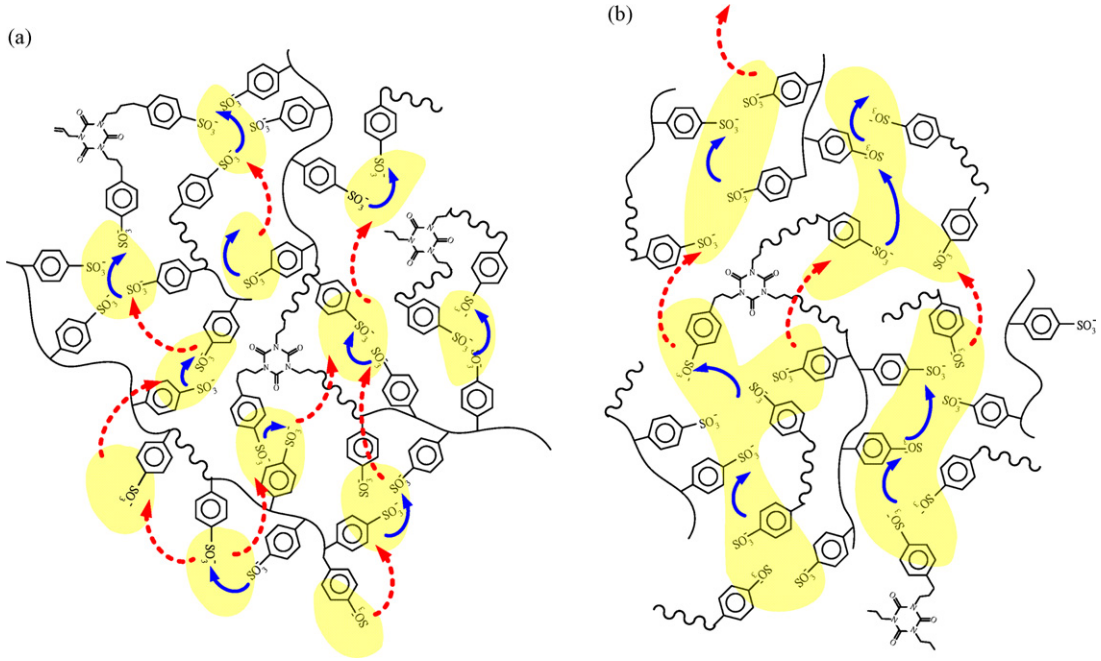

Fig. 12. (a) Schematic representation of a closed structure of the UV cured membrane. The solid arrow indicates an efficient proton transport in ionic channels (hopping mechanism) while the dash-lined arrow indicates that a less efficient proton transport through hydrophobic region. (b) A schematic representation of an open structure of the UV cured membrane.

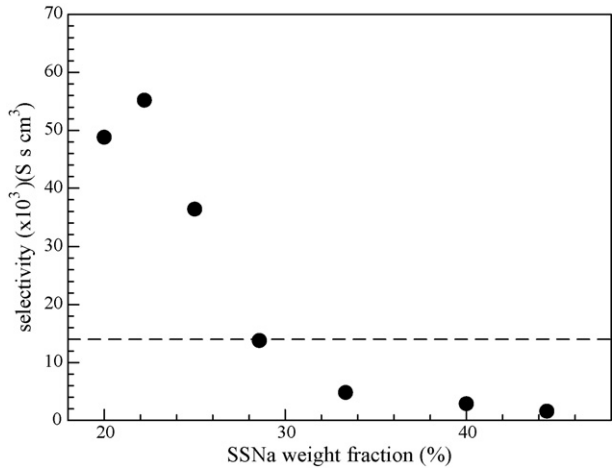

Fig. 13. Selectivity of SSNa/UAR/TAIC(2/2/X) UV cured membrane plotted as a function of SSNa weight fraction in the membrane. (●) Selectivity for the UV cured membrane and (– – –) selectivity for Nafion-117.

from Fig. 13, selectivity (Φ) values of the SSNa/UAR/TAIC membranes with SSNa weight fraction smaller than 28% are better than that of Nafion-117 indicated as a dashed line in Fig. 13. This show that a closed structure in this UV cured membrane provide better selectivity for DMFC performance.

3.6. Oxidative stability

We have also performed an oxidative stability test in Fenton's reagent (i.e., 30 wt.% H_2O_2 solution containing 30 ppm $FeSO_4$) for the SSNa/UAR/TAIC(2/2/1) polymer membrane and Nafion-117 at 30 °C. Fenton's reagent was widely used for the stability evaluation of perfluorosulfonic acid (PFSA) PEMs and other polymer membranes. The principal degradation mechanism of the polymer membranes in Fenton's reagent has been fully investigated and discussed in the literature [44]. The aqueous solution containing H_2O_2 and $FeSO_4$ forms OH radicals inside the solution, and the OH• radical may attack the polymer and decompose it [15]. However, OH radical lifetimes are short and the OH• radical cannot penetrate or diffuse into the membranes. This may be the reason for the much improved oxidative stability of these membranes. The cross-linking structure may also contribute to the stability. As listed in Table 2 SSNa/UAR/TAIC(2/2/1) membrane exhibited relatively good oxidative stability compared with that of Nafion. Therefore, using UV curing method to fabricate proton conduction membrane with good transport, mechanical and stability properties are suggested.

Table 2
The Fenton's test result of Nafion-117 and SSNa/UAR/TAIC(2/2/1) polymer membrane at 30 °C

Membranes	Oxidative time[a] (min)
Nafion	21
SSTBA/UAR/TAIC-2/2/1	18

[a] Times were recorded from the beginning to break of samples in the Fenton's reagent solution.

4. Conclusions

Novel proton exchange membranes possess an excellent combination of high proton conductivity and low methanol permeability using UV curing method successfully developed. In this study, we use a simple UV curing method to crosslink a mixture of urethane acrylate resin and triallyl isocyanate as a matrix membrane grafted with monomeric styrene sulfonate as proton conduction moiety. By modifying SSNa to obtain a liquid SSTBA, a well-mixed resin with the proton conduction moiety was obtained. It is also demonstrated that the IEC value of the membrane was found to be an important parameter in affecting water uptake, conductivity as well as the permeability of the resulting membrane. Based on the above analysis, a transition from a closed network structure to an open one was observed. The transition from a closed to an open proton conduction network was verified by the measurement of the activation energy of membrane conductivity. The activation energy in the closed structure regime was found to be around 16.5 kJ mol^{-1} which is higher than that of the open structure region of 9.6kJ mol^{-1}. This UV curing technique provides a facile method to fabricate membrane for use as PEMs for DMFCs.

Acknowledgements

The financial support from the National Science Council of Taiwan under contract no. NSC95-2218-E-002-040, NSC96-2221-E-002-145, and from the Industrial Technology Research Institute of Taiwan is greatly appreciated.

References

[1] C.C. Yang, J. Membrane Sci. 288 (2007) 51–60.
[2] V. Neburchilov, J. Martin, H. Wang, J. Zhang, J. Power Sources 169 (2007) 221.
[3] V.S. Silva, A. Mendes, L.M. Madeira, S.P. Nunes, J. Membrane Sci. 276 (2006) 126–134.
[4] J.A. Kerres, J. Membrane Sci. 185 (2001) 3–27.
[5] J. Kim, B. Kim, B. Jung, J. Membrane Sci. 207 (2002) 129–137.
[6] B. Gurau, E.S. Smotkin, J. Power Sources 112 (2002) 339–352.
[7] M. Sankir, Y.S. Kim, B.S. Pivovar, J.E. McGrath, J. Membrane Sci. 299 (2007) 8–18.
[8] A. Aramata, I. Toyoshima, M. Enyo, Electrochim. Acta 37 (1992) 1317–1320.
[9] D. Sangeetha, Eur. Polym. J. 41 (2005) 2644–2652.
[10] A. Heinzel, V.M. Barragan, J. Power Sources 84 (1999) 70–74.
[11] Y.A. Elabd, E. Napadensky, J.M. Sloan, D.M. Crawford, C.W. Walker, J. Membrane Sci. 217 (2003) 227–242.
[12] Y. Yang, F. Mikes, Y. Koike, Y. Okamoto, Macromolecules 37 (2004) 7918–7923.
[13] R.W. Kopitzke, C.A. Linkous, H.R. Anderson, G.L. Nelson, J. Electrochem. Soc. 147 (2000) 1677–1681.
[14] J.H. Chen, M. Asano, T. Yamaki, M. Yoshida, J. Membrane Sci. 269 (2006) 194–204.
[15] T. Yamaguchi, H. Zhou, S. Nakazawa, N. Hara, Adv. Mater. 19 (2007) 592.
[16] N. Carretta, V. Tricoli, F. Picchioni, J. Membrane Sci. 166 (2000) 189–197.
[17] R.A. Weiss, R.D. Lundberg, S.R. Turner, J. Polym. Sci. Pol. Chem. 23 (1985) 549–568.
[18] R.A. Weiss, S.R. Turner, R.D. Lundberg, J. Polym. Sci. Pol. Chem. 23 (1985) 525–533.
[19] S.R. Turner, R.A. Weiss, R.D. Lundberg, J. Polym. Sci. Pol. Chem. 23 (1985) 535–548.

[20] Y.S. Kim, M.A. Hickner, L. Dong, B.S. Pivovar, J.E. McGrath, J. Membrane Sci. 243 (2004) 317.
[21] D.S. Scott, W. Hafele, Int. J. Hydrogen Energ. 15 (1990) 727–737.
[22] M. Matsuguchi, H. Takahashi, J. Membrane Sci. 281 (2006) 707–715.
[23] H.Y. Cha, H.G. Choi, J.D. Nam, Y. Lee, S.M. Cho, E.S. Lee, J.K. Lee, C.H. Chung, Electrochim. Acta 50 (2004) 795–799.
[24] B.H. Lee, H.J. Kim, Polym. Degrad. Stabil. 91 (2006) 1025–1035.
[25] D. Suh, S.J. Choi, H.H. Lee, Adv. Mater. 17 (2005) 1554–1560.
[26] B.H. Lee, J.H. Choi, H.J. Kim, Jct Res. 3 (2006) 221–229.
[27] M.M. Nasef, N.A. Zubir, A.F. Ismail, M. Khayet, K.Z.M. Dahlan, H. Saidi, R. Rohani, T.I.S. Ngah, N.A. Sulaiman, J. Membrane Sci. 268 (2006) 96–108.
[28] B.S. Pivovar, Y.X. Wang, E.L. Cussler, J. Membrane Sci. 154 (1999) 155–162.
[29] J. Lobato, P. Canizares, M.A. Rodrigo, J.J. Linares, G. Manjavacas, J. Membrane Sci. 280 (2006) 351–362.
[30] V. Tricoli, J. Electrochem. Soc. 145 (1998) 3798–3801.
[31] Y. Gao, G.P. Robertson, M.D. Guiver, X.G. Ean, S.D. Mikhailenko, K.P. Wang, S. Kaliaguine, J. Membrane Sci. 227 (2003) 39–50.
[32] M. Sankir, Y.S. Kim, B.S. Pivovar, J.E. McGrath, J. Membrane Sci. 299 (2007) 8.
[33] J.L. Qiao, T. Hamaya, T. Okada, Chem. Mater. 17 (2005) 2413–2421.
[34] D.S. Kim, H.B. Park, J.W. Rhim, Y.M. Lee, J. Membrane Sci. 240 (2004) 37–48.
[35] A. Higuchi, T. Iijima, Polymer 26 (1985) 1833–1837.
[36] A. Higuchi, T. Iijima, Polymer 26 (1985) 1207–1211.
[37] B. Lafitte, L.E. Karlsson, P. Jannasch, Macromol. Rapid Comm. 23 (2002) 896–900.
[38] H.Q. Pei, L. Hong, J.Y. Lee, Langmuir 23 (2007) 5077–5084.
[39] B. Smitha, S. Sridhar, A.A. Khan, Macromolecules 37 (2004) 2233–2239.
[40] D.S. Kim, G.P. Robertson, M.D. Guiver, Y.M. Lee, J. Membrane Sci. 281 (2006) 111–120.
[41] K.D. Kreuer, Chem. Mater. 8 (1996) 610–641.
[42] D.S. Kim, B. Liu, M.D. Guiver, Polymer 47 (2006) 7871–7880.
[43] M.A. Hickner, C.H. Fujimoto, C.J. Cornelius, Polymer 47 (2006) 4238–4244.
[44] A. Bosnjakovic, S. Schlick, J. Phys. Chem. B 108 (2004) 4332–4337.